

# An animal model of hemophagocytic lymphohistiocytosis (HLH): CD8<sup>+</sup> T cells and interferon gamma are essential for the disorder

Michael B. Jordan, David Hildeman, John Kappler, and Philippa Marrack

**Hemophagocytic lymphohistiocytosis (HLH) is a rare disorder with familial and acquired forms. The familial form is associated with mutations in the perforin gene and both forms are associated with severe defects in lymphocyte cytotoxic function. We examined perforin-deficient mice as a model of HLH in order to gain insight into this poorly understood disorder. While these mice do not spontaneously develop HLH-like symptoms, we found that they manifest all of the features of HLH after infection with lymphocytic cho-**

**riomeningitic virus (LCMV). Following LCMV infection, perforin-deficient mice develop fever, splenomegaly, pancytopenia, hypertriglyceridemia, hypofibrinogenemia, and elevation of multiple serum cytokine levels, and hemophagocytosis is evident in many tissues. Investigation into how this phenotype develops has revealed that CD8<sup>+</sup> T cells, but not natural killer (NK) cells, are necessary for the development of this disorder. Cytokine neutralization studies have revealed that interferon gamma (IFN $\gamma$ ) is uniquely es-**

**sential as well. Finally, the excessive amount of IFN $\gamma$  seen in affected mice appears to be driven by increased antigen presentation to CD8<sup>+</sup> T cells. These studies provide insight into the pathophysiology of HLH, and provide new targets for specific therapeutic intervention in this fatal disorder. (Blood. 2004;104:735-743)**

© 2004 by The American Society of Hematology

## Introduction

Hemophagocytic lymphohistiocytosis (HLH) is a rare disorder with both familial and acquired forms.<sup>1-3</sup> Specific criteria for the diagnosis of this disorder have been established (Table 1).<sup>4</sup> As a familial disorder, it has an autosomal recessive inheritance and usually affects infants. As an acquired disorder, it is more variable and affects a wider age range. Acquired, or secondary, HLH has been associated with infection (most commonly with Epstein-Barr virus [EBV]), malignancy, and autoimmunity. Familial cases also commonly appear to be triggered by viral infection. While some of the features of HLH, including hemophagocytosis, can be seen in circumstances with significant immune activation, the diagnosis of this disorder is limited to situations where all of the diagnostic criteria are met.

In addition to the diagnostic features listed in Table 1, patients with HLH variably display a number of other characteristic features, such as hepatomegaly, jaundice, adenopathy, rash, seizures, and focal neurologic deficits. When assayed, patients have been found to have strikingly high serum levels of numerous cytokines including interferon gamma (IFN $\gamma$ ), tumor necrosis factor  $\alpha$  (TNF- $\alpha$ ), interleukin 6 (IL-6), IL-10, and macrophage-colony-stimulating factor (M-CSF).<sup>5-9</sup> Histologic examination of lymphoid tissues reveals a mixed infiltrate of lymphocytes and macrophages that appear highly activated. Liver biopsies typically display periportal infiltrates composed of lymphocytes and macrophages. Bone marrow biopsies may variably reveal hypoplasia or aplasia.<sup>1</sup>

Overall, patients with HLH appear to have striking activation of the immune system by both clinical and laboratory measures. It is paradoxical, therefore, that patients with both familial and secondary disease usually display a severe impairment (or complete absence) of cytotoxic function by natural killer (NK) and CD8<sup>+</sup> T cells.<sup>10,11</sup> This defect is irreversible in familial patients, but typically normalizes in patients with secondary HLH after they recover.<sup>2</sup> Furthermore, 3 distinct genetic diseases, Chediak-Higashi syndrome, Griscelli syndrome, and X-linked lymphoproliferative disorder, also produce an immune phenotype with impaired cytotoxic function and an HLH-like phase of the underlying disease process.<sup>12</sup> This common phenotype implies that the selective absence of cytotoxic function, regardless of the underlying genetic or acquired etiology, can predispose patients to develop HLH. The idea that genetic impairment of cytotoxic function may underlie familial HLH led to the discovery that a significant number of these patients have loss-of-function mutations in the gene encoding perforin.<sup>13,14</sup>

Perforin is a protein expressed in CD8<sup>+</sup> T cells and NK cells that forms holes in target cell membranes and is essential for killing via non-Fas-mediated mechanisms.<sup>15,16</sup> Perforin-deficient (pfp<sup>-/-</sup>) mice have been generated and extensively studied. In addition to other immune abnormalities, they have been noted to develop a severe, fatal course after infection with lymphocytic choriomeningitic virus (LCMV).<sup>17,18</sup> LCMV is a noncytopathic RNA virus, which is highly prevalent in wild mice.<sup>19</sup> It has been extensively

From the Integrated Department of Immunology and the Department of Pediatrics, University of Colorado Health Sciences Center, Denver, CO; Howard Hughes Medical Institute, Denver, CO; National Jewish Medical and Research Center, Denver, CO; the Cincinnati Children's Hospital and the Division of Immunobiology, University of Cincinnati, OH.

Submitted October 6, 2003; accepted February 4, 2004. Prepublished online as *Blood* First Edition Paper, April 6, 2004; DOI 10.1182/blood-2003-10-3413.

Supported by National Institutes of Health (NIH) grants AI-50802, AI-17134, AI-18785, and AI-52225, and a grant from the Histiocytosis Association of America.

An Inside *Blood* analysis of this article appears in the front of this issue.

**Reprints:** Michael Jordan, Cincinnati Children's Hospital, Immunobiology, 3333 Burnet Ave, ML 7038, Cincinnati, OH 45229-3039; e-mail: michael.jordan@cchmc.org.

The publication costs of this article were defrayed in part by page charge payment. Therefore, and solely to indicate this fact, this article is hereby marked "advertisement" in accordance with 18 U.S.C. section 1734.

© 2004 by The American Society of Hematology

**Table 1. Diagnostic criteria for HLH**

Type of diagnosis	Criteria
Clinical	Fever and splenomegaly
Laboratory	Cytopenias in at least 2 cell lineages and hypertriglyceridemia or hypofibrinogenemia
Histologic	Hemophagocytosis in bone marrow or spleen or lymph node

Adapted from Hentler et al.<sup>4</sup>

studied as a model viral infection. Like Epstein-Barr virus (EBV) infection in humans, it provokes a very vigorous CD8<sup>+</sup> T-cell response in normal mice.

The potential parallels between patients with HLH with perforin mutations and *pfp*<sup>-/-</sup> mice have been recognized since these gene defects were first described, yet no investigators have carefully examined these mice as a model of HLH. While unperturbed *pfp*<sup>-/-</sup> mice appear indistinguishable from wild-type mice, their response to LCMV is quite distinct from that of normal mice. We reasoned that LCMV-infected *pfp*<sup>-/-</sup> mice could be a good model of HLH and useful for dissecting the pathophysiology of this disorder. We found that, indeed, these mice developed all of the diagnostic and many of the characteristic features of this disorder. We have also found that the HLH-like pathology that these mice develop is dependent on CD8<sup>+</sup> T cells and IFN $\gamma$ , which is produced in response to antigenic stimulation.

## Materials and methods

### Mice, viruses, and peptide

C57Bl/6, *RAG*<sup>-/-</sup>,  $\beta$ 2m<sup>-/-</sup>, and C57Bl/6-Prf1<sup>tm1Sdz</sup> (*pfp*<sup>-/-</sup>) mice were obtained from The Jackson Laboratory (Bar Harbor, ME). B6.129S6-Pfp<sup>tm1</sup>-*Rag2*<sup>tm1</sup> (*RAG/pfp*<sup>-/-</sup>) mice were obtained from Taconic (Germantown, NY). Mice were housed in isolation facilities and euthanized if they became moribund. Temperatures were obtained using a digital thermometer placed in the hypopharynx. LCMV-WE was kindly provided by Dr J. de la Torre. Viral stocks were produced by infecting BHK-21 cells and were titered on vero cells.<sup>20</sup> Serum and tissue viral titers were obtained in the same way, using tissue homogenates. All infections of wild-type or knockout mice were via intravenous injection of virus. For most experiments, a low dose of LCMV-WE, 50 plaque-forming units (PFU), was administered. For the experiments detailed in Figure 1B-C, a more typical dose, 10<sup>7</sup> PFU, was injected because the phenotype observed in *pfp*<sup>-/-</sup> mice was more consistent at this dose. For experiments in which peptide was administered to mice, GP33 peptide was synthesized (KAVYNFATM) by the National Jewish Medical and Research Center's Molecular Resource Center, dissolved in saline, and injected (250  $\mu$ g intraperitoneally every 12 hours) starting 4 days after infection.

### Antibodies

All antibodies (except anti-CD68, which was obtained from Serotec, Raleigh, NC) were grown as tissue culture supernatants and purified over either protein A or protein G columns. The following antibodies (dose and specificity in parentheses) were administered to mice intraperitoneally every 3 days in order to deplete a cell type or neutralize a cytokine: GK1.5 (0.5 mg, CD4), YTS169 (0.5 mg, CD8), PK136 (1 mg, NK1.1), XMG1.2 (0.5 mg, IFN $\gamma$ ), MP6-XT22 (1 mg, TNF- $\alpha$ ), JES52A5 (1 mg, IL-10), C17.8 (1 mg, IL-12<sup>21</sup>; a kind gift of Dr G. Trinchieri), SK113AE-422,23 (1 mg, IL-18; a kind gift of Dr Irmgard Forster), AFS98<sup>24</sup> (1.5 mg, M-CSF; a kind gift of Dr Shinichi Nishikawa), MP1-22E9<sup>25</sup> (1.5 mg, GM-CSF), and 20LC-11.1 (1 mg, control, rat anti-DR $\beta$ 1). Each of these antibodies was administered at doses equal to or greater than those reported to deplete or neutralize their respective targets. To check for efficacy, serum samples were assayed for the respective cytokine, or spleen cells were examined by flow cytometry. The following anti-LCMV antibodies were a kind gift of

Dr Michael Buchmeier (the Scripps Research Institute): WE-36.1, WE-258.4, WE-197.4.<sup>26</sup> Mice were injected intraperitoneally with 2 mg of each antibody between 4 and 6 days after infection in order to decrease viral burden.

### Histology, flow cytometry, and intracellular cytokine staining

Tissues and cytospin slides were fixed in B5/formalin and paraffin embedded for hematoxylin and eosin stain via standard protocols. For preparation of cell suspensions, tissues were digested in collagenase D (Roche, Milan, Italy) and DNase (Sigma, St Louis, MO).<sup>27</sup> Staining of macrophages for flow cytometry was performed at 4°C in the presence of 5 mM EDTA [ethylenediaminetetraacetic acid] to prevent cell loss due to adherence. For cytospins, spleen or bone marrow cell suspensions were centrifuged over ficoll gradients to separate high-density cells, which were spun onto slides. Major histocompatibility complex (MHC)-peptide tetramers (D<sup>b</sup>-GP33) were produced as covalently linked MHC-peptide molecules in baculovirus-infected insect cells, biotinylated, and assembled around streptavidin-phycoerythrin.<sup>28</sup> For intracellular cytokine staining, cells were cultured with GP33 peptide (10  $\mu$ g/mL) in the presence of monensin for 6 hours, fixed and permeabilized with cytofix/cytoperm (PharMingen, San Diego, CA), and stained with Oregon green (Molecular Probes, Eugene, OR)-labeled anti-IFN $\gamma$ . Images were obtained using an Olympus BX40 microscope (Melville, NY) equipped with a Kodak MDS120 digital camera (Eastman Kodak, Rochester, NY), using the 100 $\times$  (numerical aperture 1.3) oil objective. Images were acquired using NIH Scion Image software, version 1.62 (developed at the National Institutes of Health, obtained at <http://rsb.info.nih.gov/nih-image/>).

### Clinical laboratory tests and ELISA

Serum triglyceride and plasma fibrinogen assays were performed by IDEXX (Sacramento, CA). All triglyceride determinations were performed on serum samples from mice that were fasted overnight. Complete blood counts were determined by the clinical laboratory at National Jewish Medical and Research Center using a Sysmex NE1500 (Sysmex, Long Grove, IL). All serum cytokine levels were determined by using enzyme-linked immunosorbent assay (ELISA) kits obtained from R&D Systems

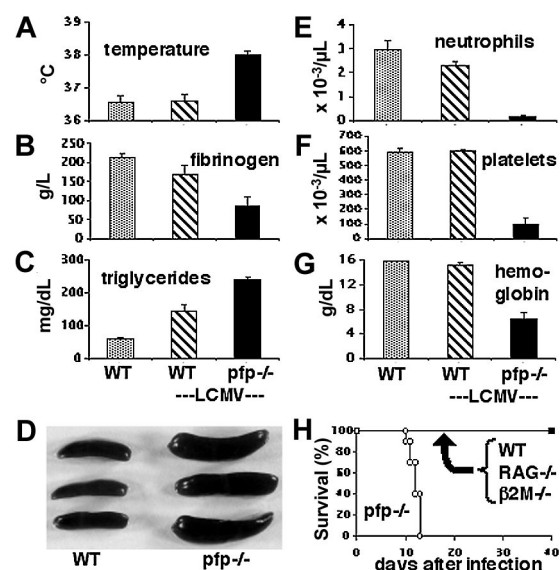


**Figure 1. LCMV-infected *pfp*<sup>-/-</sup> mice display clinical and laboratory features of HLH.** Wild-type and *pfp*<sup>-/-</sup> mice were infected with LCMV-WE. Eight to 12 days after infection, these animals and uninfected wild-type mice were assayed for (A) temperature, (B) plasma fibrinogen, (C) serum triglycerides, (D) spleen size, (E) peripheral blood neutrophil counts, (F) platelet counts, and (G) hemoglobin. The spleen photo in panel D portrays uninfected wild-type spleens and infected *pfp*<sup>-/-</sup> spleens. (H) Survival of mice was monitored after LCMV infection of wild-type, *RAG*<sup>-/-</sup>,  $\beta$ 2m<sup>-/-</sup>, and *pfp*<sup>-/-</sup> mice. Data shown ( $\pm$  standard error) are representative of at least 2 experiments with at least 3 mice in each group.

(Minneapolis, MN) per the manufacturer's instructions. For each cytokine, sera from uninfected wild-type and pfp<sup>-/-</sup> mice were assayed and found to contain undetectable levels, except IL-6 and IL-18, which had very low levels (< 20% of infected, wild-type mice).

## Results

### LCMV-infected pfp<sup>-/-</sup> mice display clinical and laboratory features of HLH

We examined LCMV-infected pfp<sup>-/-</sup> mice to determine whether they displayed the clinical and laboratory criteria, shown in Table 1, that are required for the diagnosis of HLH. Early after infection with LCMV, the physical appearance of both wild-type and pfp<sup>-/-</sup> mice was unaffected. By about 10 days after infection, however, the pfp<sup>-/-</sup> mice displayed decreased activity, ruffled fur, and hunched posture. When we examined mice at this time, we found that only pfp<sup>-/-</sup> mice were febrile (Figure 1A). Whereas wild-type mice developed a brief febrile response early after LCMV infection (data not shown), the pfp<sup>-/-</sup> mice had prolonged temperature elevation. At 8 to 10 days after infection, pfp<sup>-/-</sup> mice also developed hypofibrinogenemia (Figure 1B), and hypertriglyceridemia (Figure 1C), compared with either resting or LCMV-infected wild-type mice. Similar to wild-type mice, pfp<sup>-/-</sup> mice also developed splenomegaly after LCMV infection (Figure 1D). Unlike wild-type mice, however, pfp<sup>-/-</sup> mice became uniformly pancytopenic by 10 days after infection (Figure 1E-G). Without specific intervention, these mice died within 2 weeks of infection (Figure 1H), similar to untreated familial HLH patients, who die fairly rapidly without treatment.<sup>29</sup> This fate is distinctly different from that of wild-type, lymphocyte-deficient (RAG<sup>-/-</sup>), or CD8<sup>+</sup> T-cell-deficient ( $\beta$ 2m<sup>-/-</sup>) mice that do not normally die after infection (Figure 1H). These mice survive infection even though lymphocyte-deficient and CD8<sup>+</sup> T-cell-deficient mice fail to clear LCMV infection, similar to pfp<sup>-/-</sup> mice. In summary, LCMV-infected pfp<sup>-/-</sup> mice display all of the diagnostic clinical and laboratory features of HLH.

### LCMV-infected pfp<sup>-/-</sup> mice display histopathologic features of HLH

In addition to specific clinical and laboratory criteria, the diagnosis of HLH is dependent on the demonstration of hemophagocytosis in at least one of several tissues (Table 1). We examined the tissues of LCMV-infected pfp<sup>-/-</sup> and wild-type mice for this and other signs of HLH. Prior to and early after infection, these 2 groups of mice were indistinguishable (data not shown). By days 10 to 12 after infection, however, pfp<sup>-/-</sup> mice displayed multiple histologic changes consistent with HLH (Figure 2A, with tissues from uninfected wild-type mice for comparison). First, lymph node architecture was profoundly deranged. Disorganized infiltrates of macrophages and activated lymphocytes replaced the normal follicular structure of lymph nodes. Some specimens also displayed necrotic changes. Second, splenic architecture was altered. The red pulp was expanded and the white pulp appeared somewhat chaotic with a prominent infiltrate of macrophages and activated lymphocytes. Third, liver sections revealed prominent periportal infiltrates. Fourth, bone marrow sections displayed severe hypoplasia. Fifth, while examination of the meninges 12 days after infection revealed minimal infiltrates, a prominent mononuclear infiltrate was present along the dura in pfp<sup>-/-</sup> mice by about day 30 after infection. In order to survive to this late time point, mice were given specific

therapy to partially alleviate their condition (see "Materials and Methods"). High-power examination of sections or cytopins from each of these tissues revealed hemophagocytic macrophages (Figure 2A). While this feature was consistently present in pfp<sup>-/-</sup> mice (and rarely, if ever, found in wild-type mice), its histologic prominence was somewhat variable.

To further examine these changes in tissue cellularity, flow cytometry was performed. Relative macrophage infiltrates, as expressed by percent of cells that were CD68<sup>+</sup> in spleen, liver, and bone marrow, are shown in Figure 2B. These percentages were derived by gating on live cells and specifically excluding hepatocytes in the liver cell suspensions. While the relative increase in macrophages is readily apparent, the absolute increase is relatively modest in the bone marrow due to hypoplasia, and in the spleen due to overall decreased cellularity and specific loss of B cells (data not shown).

To further characterize the macrophage populations seen in mice after LCMV infection, we performed flow cytometry on bone marrow specimens obtained 12 days after infection (Figure 2C). We found that, compared with wild-type mice, macrophages (CD68<sup>+</sup>) from pfp<sup>-/-</sup> mice have greatly increased levels of MHC class II on their surface, a classic marker of activation. Correlating with this change was a significant increase in IFN $\gamma$ -secreting CD8<sup>+</sup> cells in the bone marrow of pfp<sup>-/-</sup> mice (Figure 6A).

### LCMV-infected pfp<sup>-/-</sup> mice display striking elevations of serum cytokine levels

Much attention has been paid to derangements of serum cytokine levels in patients with HLH. These patients have been found to have elevations in the levels of a number of cytokines including TNF- $\alpha$ , IFN $\gamma$ , IL-6, IL-10, IL-18, and M-CSF.<sup>1,2</sup> Many investigators have speculated that these changes may be an important part of the pathogenesis of this disorder. Because LCMV-infected pfp<sup>-/-</sup> mice appeared so similar to patients with HLH in other aspects of the disorder, we hypothesized that they might have similar derangements of serum cytokine levels. We assayed serum samples from both wild-type and pfp<sup>-/-</sup> mice 12 days after infection (day 6 for interferon alpha [IFN $\alpha$ ]) for each of the cytokines listed above and IFN $\alpha$ . Pfp<sup>-/-</sup> mice displayed dramatically elevated serum levels for each of these cytokines (Figure 3). We assayed day-12 sera because at this time pfp<sup>-/-</sup> mice displayed all of the features of HLH. We found that serum IFN $\alpha$  levels peaked early (at or before day 3) and are undetectable by day 4 or 5 in wild-type mice (data not shown). Pfp<sup>-/-</sup> continue to have increased levels of IFN $\alpha$  until days 6 to 8 (Figure 3). Serum from uninfected wild-type and pfp<sup>-/-</sup> mice was assayed and found to have very low or undetectable levels of all of these cytokines. Unlike the other cytokines shown in Figure 3, IL-1 $\beta$  is notably not elevated in human patients with HLH. We assayed the serums of both wild-type and pfp<sup>-/-</sup> mice at either day 6 or day 12 after LCMV infection, and could find no detectable IL-1 $\beta$  in the serum of either group (data not shown).

### Both CD8<sup>+</sup> T cells and IFN $\gamma$ are necessary for the development of an HLH-like disorder in LCMV-infected pfp<sup>-/-</sup> mice

In order to determine which cell types are necessary for the development of HLH-like pathology after infection with LCMV, we conducted a series of cell depletion experiments (Figure 4A). Six days after infection we administered antibodies to deplete CD4<sup>+</sup>, CD8<sup>+</sup>, or NK1.1<sup>+</sup> cells. We found that most pfp<sup>-/-</sup> mice depleted of CD8<sup>+</sup> cells survived infection, but that none of the

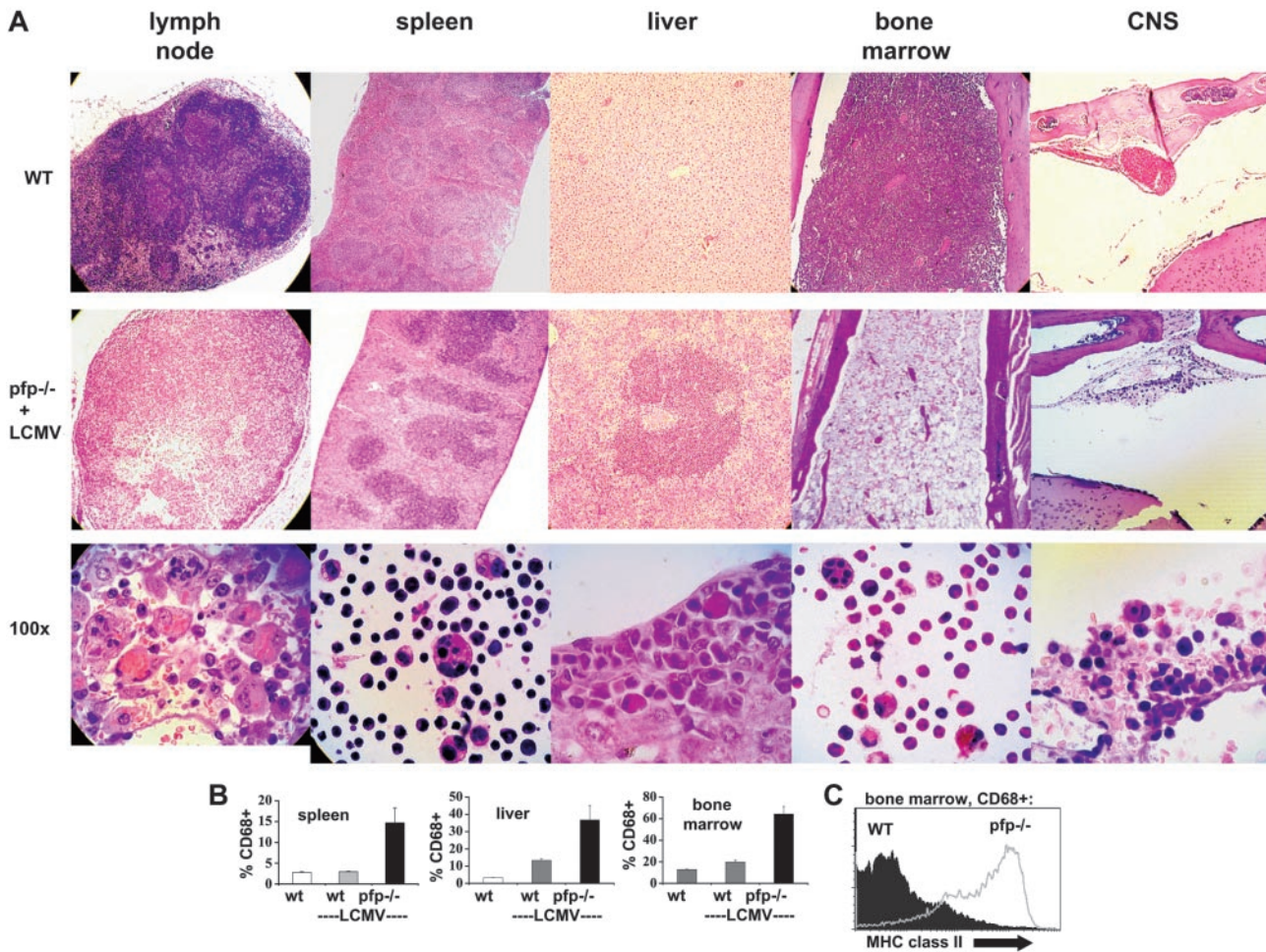


**Figure 2. LCMV-infected  $pfp^{-/-}$  mice display histopathologic features of HLH.** (A) Tissue sections from uninfected wild-type mice or LCMV-infected  $pfp^{-/-}$  mice were stained with hematoxylin and eosin. All images are of paraffin-embedded tissue, except the high-power views of spleen and bone marrow cells, which are cytopsins. All  $pfp^{-/-}$  samples were taken from mice 12 days after infection, except for the central nervous system (CNS) sections which were taken from mice infected 30 days previously and treated with anti-LCMV antibodies (Figure 6). (B) Tissues from wild-type mice (with and without LCMV infection) and LCMV-infected  $pfp^{-/-}$  mice were analyzed by flow cytometry for the relative content of macrophage-lineage cells (% CD68<sup>+</sup>). Error bars represent SEM. (C) CD68<sup>+</sup> cells from the bone marrow of wild-type and  $pfp^{-/-}$  mice infected with LCMV 12 days previously were stained for MHC class II. Data ( $\pm$  standard error) are representative of at least 2 experiments with at least 3 mice in each group.

animals depleted of CD4 or NK cells survived. In addition to depletion experiments, double knockout mice deficient for both T/B lymphocytes and perforin ( $RAG/pfp^{-/-}$ ) were infected with LCMV. Similar to  $RAG^{-/-}$  and  $\beta 2m^{-/-}$  mice, these mice did not

die. Together, these depletion and genetic experiments indicate that CD8<sup>+</sup> T cells are essential for the development of an HLH-like syndrome.

Next, we sought to determine which cytokines contributed to the development of HLH-like pathology in LCMV-infected  $pfp^{-/-}$  mice. This question is complicated by the fact that a wide range of cytokine levels are elevated in patients with HLH and in these mice. To screen candidate cytokines, we administered neutralizing antibodies beginning 6 days after infection and monitored survival of mice. Surprisingly, we found that neutralizing multiple cytokines, including TNF- $\alpha$ , IL-12, IL-18, M-CSF, and GM-CSF had no effect on survival (Figure 4B). However, if IFN $\gamma$  was neutralized, most mice survived, indicating that this cytokine is essential for the development of HLH-like pathology in LCMV-infected  $pfp^{-/-}$  mice. Even though mortality is directly linked to IFN $\gamma$ , it is not surprising that neutralization of IL-12 did not affect survival. Orange and Biron<sup>30</sup> demonstrated that the IFN $\gamma$  response to LCMV is completely independent of IL-12. Less is known, however, about the relationship between IL-18 and IFN $\gamma$  after LCMV infection. Pien et al reported that IL-18<sup>-/-</sup> mice produce about 50% less IFN $\gamma$  (as measured in serum) than wild-type mice.<sup>31</sup> We have found that IL-18 levels are increased in  $pfp^{-/-}$  mice at day 8 after infection, but this elevation is mild compared with day 12 levels, or

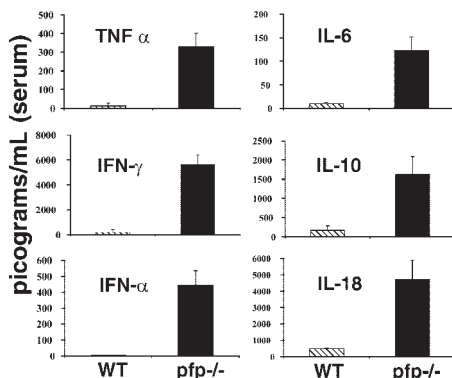


**Figure 3. LCMV-infected  $pfp^{-/-}$  mice display striking elevations of serum cytokine levels.** Serum cytokine levels from either wild-type or  $pfp^{-/-}$  mice infected with LCMV are shown. All assays were performed on sera obtained 12 days after infection, except IFN $\alpha$ , which was assayed on sera from mice infected 6 days previously. Data ( $\pm$  standard error) are representative of at least 2 experiments with at least 3 mice in each group.

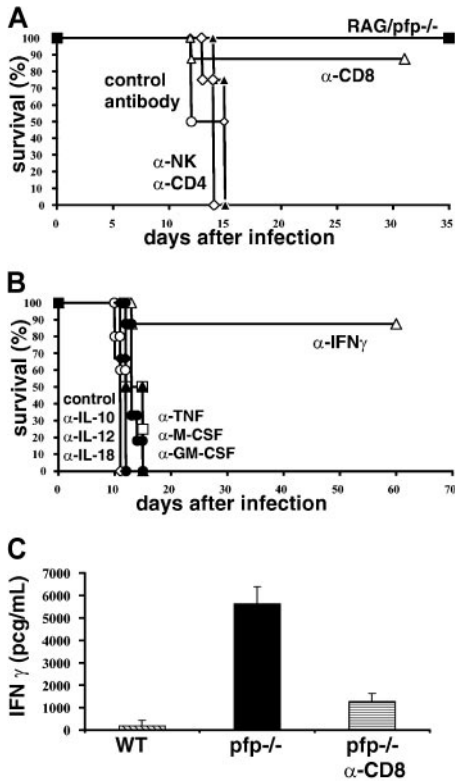


**Figure 4.** Both CD8<sup>+</sup> T cells and IFN $\gamma$  are necessary for the development of an HLH-like disorder in LCMV-infected pfp<sup>-/-</sup> mice. (A) Pfp<sup>-/-</sup> mice were treated with control, CD4, CD8, or NK cell-depleting antibodies starting 6 days after LCMV infection and were monitored for survival. RAG/pfp<sup>-/-</sup> mice were infected with LCMV and monitored for survival. (B) Pfp<sup>-/-</sup> mice were infected with LCMV and given cytokine-neutralizing antibodies (against TNF- $\alpha$ , IFN $\gamma$ , M-CSF, GM-CSF, IL-10, IL-12, and IL-18) starting on day 6 and were monitored for survival. (C) Serum IFN $\gamma$  levels were assayed on day 12 from wild-type, control antibody-treated pfp<sup>-/-</sup> mice, and pfp<sup>-/-</sup> mice that had received anti-CD8 antibody. Data ( $\pm$  standard error) are representative of at least 2 experiments with at least 3 mice in each group.

compared to the elevation of IFN $\gamma$  levels at any time point (data not shown and Figure 5).

Linking the findings in Figure 4A-B together, we found that CD8 depletion of LCMV-infected pfp<sup>-/-</sup> mice substantially lowered serum IFN $\gamma$  levels (Figure 4C). Furthermore, when we looked at which cells were secreting IFN $\gamma$  ex vivo, either spontaneously or with peptide stimulation, we found that almost all of the cells that were IFN $\gamma$ <sup>+</sup> were also CD8<sup>+</sup> (data not shown and Figure 6). Thus, the HLH-like disease seen after LCMV infection in pfp<sup>-/-</sup> mice is dependent on IFN $\gamma$ , which appears to be secreted by CD8<sup>+</sup> T cells.

**IFN $\gamma$  is intimately associated with the development of HLH-like pathology in LCMV-infected pfp<sup>-/-</sup> mice**

Because neutralizing IFN $\gamma$  had such a dramatic effect on survival, we investigated its role further. A time course of serum IFN $\gamma$  levels in wild-type and pfp<sup>-/-</sup> mice revealed that the latter mice have greatly elevated and prolonged serum levels of this cytokine (Figure 5A). We next determined whether IFN $\gamma$  was necessary for the development of specific aspects of HLH-like pathology in these mice. We found that if IFN $\gamma$  was neutralized starting 6 days after infection, histiocytic infiltrates did not develop like they did in control antibody-treated pfp<sup>-/-</sup> mice (Figure 5B). We also found that peripheral blood cytopenias failed to develop if IFN $\gamma$  was blocked (Figure 5C). Thus, IFN $\gamma$  is necessary for the development of multiple features of the HLH-like disorder seen in pfp<sup>-/-</sup> mice.

**Excessive IFN $\gamma$  production in LCMV-infected pfp<sup>-/-</sup> mice is driven by persistent antigen presentation to CD8<sup>+</sup> T cells**

Next, we investigated what was causing this excessive production of IFN $\gamma$ . We postulated that this excess could be caused by (1) a dramatic increase in antigen-responsive CD8<sup>+</sup> T cells, (2) an abnormally vigorous responsiveness of pfp<sup>-/-</sup> T cells, (3) a normal response to abnormally elevated or persistent levels of antigen, or (4) a combination of these factors. When we examined the total number of CD8<sup>+</sup> T cells in pfp<sup>-/-</sup> mice at various times after infection, in spleen, liver, bone marrow, and lymph node the number was usually similar or mildly elevated, compared with that of wild-type mice (data not shown). However, if we assayed the number of antigen-specific CD8<sup>+</sup> T cells in pfp<sup>-/-</sup> mice using an MHC-peptide staining reagent (D<sup>b</sup>-GP33), we found that this number was typically elevated 2- to 5-fold over that of wild-type mice in bone marrow, liver, and spleen (Figure 6A and data not shown). Staining for intracellular IFN $\gamma$  after GP33 peptide stimulation gave similar results (Figure 6A). When we examined the number of antigen-specific CD4<sup>+</sup> T cells in pfp<sup>-/-</sup> mice using MHC-peptide tetramers, we saw increases that were similar to those in the CD8<sup>+</sup> T-cell compartment (data not shown).

While this increase in the number of antigen-specific CD8<sup>+</sup> (and CD4<sup>+</sup>) T cells could account for some of the increased production of IFN $\gamma$ , it could not account for all (or most) of it. Although the number of antigen-specific CD8<sup>+</sup> T cells was increased several fold, the serum level of IFN $\gamma$  was increased between 10- and 1000-fold after infection, compared with wild-type mice (Figure 5A).

To assess whether pfp<sup>-/-</sup> T cells were abnormally responsive to stimulation, we examined cytokine production by these cells, using intracellular staining. When we stimulated spleen cells from mice infected 6 to 10 days previously, we found that IFN $\gamma$  production was less, on a per-cell basis, in pfp<sup>-/-</sup> compared with wild-type CD8<sup>+</sup> T cells (Figure 6B). Similar results were seen with both peptide stimulation and anti-CD3 stimulation (data not shown). One possible explanation for these surprising data is that they reflect exhaustion or down-regulation of IFN $\gamma$  production subsequent to recent in vivo stimulation.<sup>32,33</sup> Consistent with this

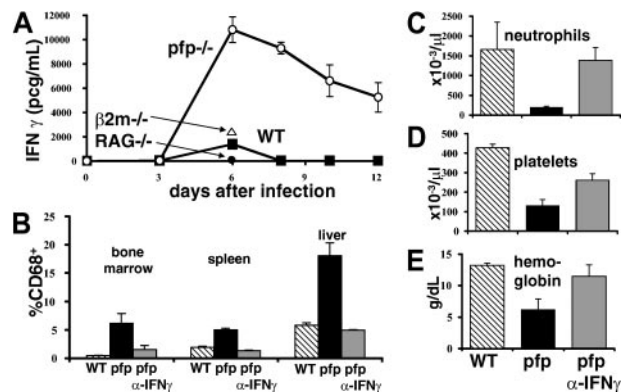


**Figure 5.** IFN $\gamma$  is intimately associated with the development of HLH-like pathology in LCMV-infected pfp<sup>-/-</sup> mice. (A) Serum IFN $\gamma$  levels were assayed in wild-type, pfp<sup>-/-</sup> RAG<sup>-/-</sup>, and  $\beta$ 2m<sup>-/-</sup> mice at various times after LCMV infection. (B) Twelve days after LCMV infection, tissues were analyzed by flow cytometry for the relative percent of macrophage-lineage (CD68<sup>+</sup>) cells in wild-type, pfp<sup>-/-</sup>, and pfp<sup>-/-</sup> mice that had received anti-IFN $\gamma$  antibody. Peripheral blood (C) neutrophil, (D) platelet, and (E) hemoglobin levels were assayed in the same groups. Data ( $\pm$  standard error) are representative of at least 2 experiments with at least 3 mice in each group.

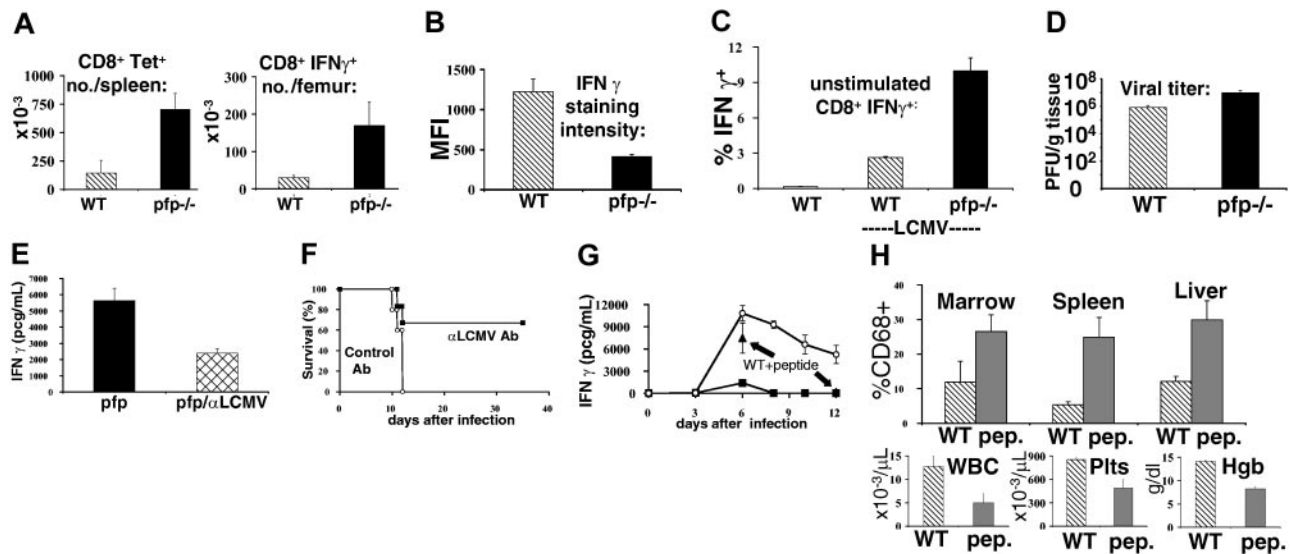


**Figure 6. Excessive IFN $\gamma$  production in LCMV-infected  $pfp^{-/-}$  mice is driven by persistent antigen presentation to CD8 $^{+}$  T cells.** (A) Ten days after LCMV infection, antigen-specific CD8 $^{+}$  T cells from wild-type and  $pfp^{-/-}$  mice were quantitated by MHC-peptide tetramer (D $^b$ -GP33) staining and intracellular IFN $\gamma$  staining (after stimulation with GP33 peptide). (B) Relative staining intensity for IFN $\gamma$  was quantitated in wild-type and  $pfp^{-/-}$  CD8 $^{+}$  T cells after *in vitro* stimulation with peptide (GP33). MFI indicates mean fluorescence intensity. (C) Spontaneous IFN $\gamma$  production by CD8 $^{+}$  T cells obtained 6 days after LCMV infection was assessed in wild-type and  $pfp^{-/-}$  mice by intracellular staining in the absence of stimulating peptide. (D) Viral titers were measured in wild-type and  $pfp^{-/-}$  spleens 6 days after LCMV infection. (E) Serum IFN $\gamma$  levels were assayed at day 12 in  $pfp^{-/-}$  mice that had been given either control or LCMV-neutralizing antibody 4 to 6 days after infection. (F) Survival was monitored in these same mice. (G) Wild-type mice were given GP33 peptide (250 mcg every 12 hours, intraperitoneally) starting 4 days after LCMV infection. Serum IFN $\gamma$  levels were assayed at days 6 and 12 and plotted with the time course from Figure 5A for comparison. (H) Relative macrophage infiltrates (% CD68 $^{+}$ ) in various tissues and blood cellularity were compared between wild-type mice that did or did not receive GP33 peptide after LCMV infection (assayed at day 12). WBC indicates white blood cells; Plts, platelets; and Hgb, hemoglobin. Data ( $\pm$  standard error) are representative of at least 2 experiments with at least 3 mice in each group.

interpretation, we found that the number of spontaneously IFN $\gamma$ -producing (without stimulation) CD8 $^{+}$  T cells was increased in  $pfp^{-/-}$  mice (Figure 6C). Thus, our data suggested that ongoing antigenic stimulation, and not a cell autonomous abnormality of  $pfp^{-/-}$  CD8 $^{+}$  T cells, was contributing to increased cytokine secretion.

To investigate the possibility that abnormal antigen presentation was contributing to the abnormal IFN $\gamma$  seen in  $pfp^{-/-}$  mice, we first assayed the viral burden in these mice. At later time points, after wild-type mice have cleared LCMV infection and  $pfp^{-/-}$  mice have failed to do so, this is an obvious potential contributor. However, the IFN $\gamma$  levels of these 2 groups diverged as early as day 6 after infection. We measured virus in the spleens of these mice at this time to see if the viral burden was different. We found that while spleens from both groups of mice contained significant amounts of virus at day 6, the  $pfp^{-/-}$  mice harbored nearly 10-fold more infectious virus (Figure 6D).

In order to determine whether excessive antigen presentation was necessary for HLH-like pathology, we administered LCMV-neutralizing antibodies to  $pfp^{-/-}$  mice 4 to 6 days after infection. These antibodies have been shown to decrease viral burden *in vivo* and in our mice they completely neutralized serum virus (data not shown).<sup>34,35</sup> We found that administration of these antibodies decreased serum IFN $\gamma$  levels in  $pfp^{-/-}$  mice at day 12 after infection (Figure 6E), and allowed for prolonged survival in a substantial portion of mice (Figure 6F). While disease was mitigated in these mice, it was not eliminated (Figure 2A), consistent with the inability of antibody to completely clear LCMV infection.

To determine whether prolonged/excessive antigen presentation is *sufficient* to cause elevated serum IFN $\gamma$  levels and an HLH-like process, we administered synthetic GP33 peptide (the dominant CD8 $^{+}$  T-cell-stimulating epitope) to wild-type mice starting 4 days after infection with LCMV. We found that, with

this persistent antigen administration, IFN $\gamma$  levels were substantially elevated in these mice at day 6 after infection, similar to  $pfp^{-/-}$  mice (Figure 6G). Furthermore, between days 8 and 12, these mice developed the hunched posture, decreased mobility, and ruffled fur that is characteristic of  $pfp^{-/-}$  mice after LCMV infection (data not shown). By day 12, they had developed depressed peripheral blood counts and relative increases in macrophages in several tissues (Figure 6H), though these changes were milder than those typically seen in  $pfp^{-/-}$  mice. Despite persistent administration of peptide, however, these mice down-regulated their IFN $\gamma$  response by day 12 to near-normal levels (Figure 6G). Additionally, no wild-type mice in these experiments died (data not shown). Thus, persistent antigen in wild-type animals was able to partially recreate the pathology seen in  $pfp^{-/-}$  mice after LCMV infection.

In summary, these data indicate that increased IFN $\gamma$  production observed in  $pfp^{-/-}$  mice after LCMV infection is largely due to elevated/prolonged antigen presentation. An increase in antigen-specific CD8 $^{+}$  T cells is probably contributing as well, but we have seen little evidence for a cell autonomous defect in these cells.

## Discussion

The studies described in this paper represent the first thorough examination of LCMV-infected  $pfp^{-/-}$  mice as a model for human HLH. When infected with LCMV, these mice develop fever, splenomegaly, pancytopenia, hypertriglyceridemia, hypofibrinogenemia, and hemophagocytosis. Furthermore, they develop other histologic features characteristic of HLH: activated lymphohistiocytic infiltrates, splenic/lymph node follicular depletion, periportal infiltrates, bone marrow hypoplasia, and meningeal infiltrates.

Their serum cytokine profiles are also very similar to those of human patients with HLH.

This murine model of HLH has yielded insights into how HLH may develop. In this model, IFN $\gamma$  produced by CD8<sup>+</sup> T cells is uniquely essential for the development of HLH-like pathology. Notably, NK cells and a variety of cytokines, including TNF- $\alpha$ , are not necessary. Pathologic levels of IFN $\gamma$  are promoted by excessive antigenic stimulation of CD8<sup>+</sup> T cells.

The idea that perforin-dependent cytotoxic function has an important immunoregulatory role is not a new one. Investigators noticed years ago that after infection with high doses of LCMV-WE, marginal zone macrophages were depleted in a CD8<sup>+</sup> T-cell-dependent fashion, and that this depletion was linked to suppression of subsequent antibody responses.<sup>36</sup> More recently, other investigators have shown that CD8<sup>+</sup> T cells can kill exogenously administered dendritic cells, presumably via perforin-dependent mechanisms, and thus limit T-cell priming by these cells.<sup>37</sup> Furthermore, several groups have demonstrated that pfp<sup>-/-</sup> mice can mount exaggerated immune responses in certain circumstances.<sup>17,18,38-40</sup>

While this paper is the first one to specifically examine the features of LCMV-infected pfp<sup>-/-</sup> mice relevant to HLH, other investigators have described pathologic responses of pfp<sup>-/-</sup> mice to LCMV infection.<sup>17,18,40</sup> Binder et al<sup>17</sup> first noted the unusual mortality in these mice and linked IFN $\gamma$  to bone marrow dysfunction. More recently, Badovinac et al<sup>40</sup> described exaggerated CD8<sup>+</sup> T-cell responses and death after LCMV infection of pfp<sup>-/-</sup> mice. In their system, they utilized pfp<sup>-/-</sup> mice on the BALB/c strain, which is known to be a weaker producer of IFN $\gamma$  than the C57BL/6 strain. Additionally, they infected the mice with the Armstrong strain of LCMV, which is known to stimulate a less vigorous IFN $\gamma$  response than the WE strain of LCMV.<sup>31</sup> Not surprisingly, naive pfp<sup>-/-</sup> mice in Badovinac et al's system did not die after infection with LCMV. However, if they first infected the animals with a recombinant *Listeria monocytogenes* strain expressing LCMV antigen, and then later challenged them with LCMV, the pfp<sup>-/-</sup> mice mounted an exaggerated CD8<sup>+</sup> T-cell response and died within 8 days. The effect of this vaccination was to generate a more robust IFN $\gamma$  response and, thus, drive the phenotype of their mice closer to the phenotype we observe in our experimental our system. Similar to our data, if Badovinac et al administered neutralizing anti-IFN $\gamma$  antibody, all of the mice survived.

LCMV infection of pfp<sup>-/-</sup> mice appears to be unique as a murine model of HLH. Multiple other investigators have examined viral infection of pfp<sup>-/-</sup> mice. No excess mortality is reported after infection with murine cytomegalovirus, murine gamma-herpesvirus 68, vaccinia virus, or vesicular stomatitis virus.<sup>41-43</sup> There are conflicting reports regarding mortality after infection with influenza A. Topham et al<sup>44</sup> report no mortality, while Liu et al<sup>45</sup> (using a different strain) report approximately 50% mortality. Interestingly, the latter group reports significantly higher production of IFN $\gamma$  in the lungs of pfp<sup>-/-</sup> mice compared with wild-type mice. Although none of these groups were looking for specific signs of HLH, the absence of mortality (with the possible exception of influenza) indicates that these viral infections are probably not triggering an HLH-like condition. Why, therefore, is LCMV unique? One possible explanation is that vaccinia, vesicular stomatitis virus, and influenza are all cleared in a normal or near-normal fashion, thus limiting antigenic stimulation. The 2 other viruses that are not contained in a normal fashion, murine cytomegalovirus (MCMV) and murine gamma-herpesvirus 68, are both herpes family viruses

with sophisticated mechanisms of immune evasion. MCMV, for instance, is known to disable macrophages as antigen-presenting cells and inhibit their responsiveness to IFN $\gamma$ .<sup>46,47</sup>

In light of our data, and work by other investigators, we propose the following model for the pathophysiology of HLH (Figure 7). In a normal immune response, foreign antigen is presented by antigen-presenting cells (APCs) to CD4<sup>+</sup> and CD8<sup>+</sup> T cells. In response, T cells are stimulated to proliferate and differentiate. As part of this differentiation, T cells produce a variety of cytokines which can activate APCs and further promote presentation of antigen. In particular, CD8<sup>+</sup> T cells are an important source of IFN $\gamma$ , which is a classical activator of macrophages. As the CD8<sup>+</sup> T cells acquire the ability to secrete cytokines, however, they also acquire cytotoxic function and begin to kill virally infected cells (including macrophages and other APCs) via perforin-dependent mechanisms. This killing, perhaps along with another undefined function of perforin, acts as a negative regulator of these mutually stimulatory interactions. In this way, the selective loss of cytotoxic function creates an imbalance in the immune system, promoting abnormal and excessive production of T-cell-derived cytokines, such as IFN $\gamma$ . This excessive IFN $\gamma$  response is quite toxic and, in ways that are not yet defined, leads to the characteristic histologic and clinical features of HLH, including hemophagocytosis. In a viral infection such as with LCMV or EBV, the CD8<sup>+</sup> T-cell cytotoxic and IFN $\gamma$  responses are very vigorous and the potential for immune-mediated pathology is substantial.

Two important aspects of this model are not yet fully understood. First, precisely how perforin contributes to the down-regulation of the CD8<sup>+</sup> T-cell IFN $\gamma$  response is not clear. Does it simply cause a decrease in the total antigen load or is the *quality* of antigen presentation changed, for instance, by modulation or destruction of a particular APC subset? Our data with exogenously administered antigen (Figure 6) imply that this phenomenon is more complex than a simple decrease of antigen load. As stated above, other investigators have found evidence for destruction of APCs by CD8<sup>+</sup> T cells in some circumstances.<sup>36,37</sup> When we examined mice 6 to 8 days after infection, while cytotoxic responses are near maximal, we did not find wholesale destruction of macrophages/dendritic cells in wild-type mice, or a clearly different fate for these cells in pfp<sup>-/-</sup> mice (data not shown). Although pfp<sup>-/-</sup> mice have exaggerated macrophage infiltrates 12

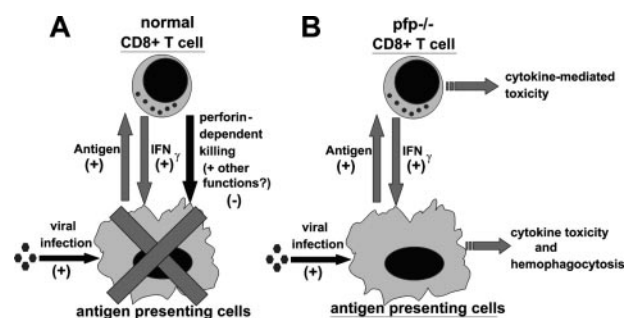


**Figure 7. Proposed model of the pathophysiology of HLH.** (A) During a normal immune response, presentation of antigen promotes CD8<sup>+</sup> T-cell responses. In return, CD8<sup>+</sup> T cells secrete IFN $\gamma$ , which activates antigen-presenting cells and further promotes antigen presentation. This positive feedback loop is restrained by perforin-dependent mechanisms. It remains unclear whether this occurs via specific destruction of professional antigen-presenting cells, general destruction of virally infected cells, or additional mechanisms. (B) In LCMV-infected pfp<sup>-/-</sup> mice, the failure of perforin-dependent mechanisms allows for spiraling immune activation and excessive secretion of IFN $\gamma$ . This leads to the development of an HLH-like syndrome.

days after infection, this occurs in the context of persistent infection and inflammation.

Second, how high IFN $\gamma$  levels lead to HLH-like pathology is not yet clear. Because it is known to be toxic to hematopoietic cells, it is easy to imagine how it may contribute to the destruction of bone marrow cells.<sup>48</sup> On the other hand, how it contributes to the appearance of hemophagocytic macrophages is not understood. While IFN $\gamma$  is a classical activator of macrophages, it is not known to promote phagocytosis.<sup>49</sup> Furthermore, the specific causal role of macrophages in producing the signs and symptoms of HLH is not yet established. It is possible that the hemophagocytic macrophages observed in both mice and humans may simply be a result of, and not a cause of, HLH pathophysiology.

HLH is a disorder with diverse genetic and environmental associations. The mouse model described in this work utilizes a virally infected, genetically modified mouse strain, thus combining elements of both familial and secondary HLH. Because of the

apparent diversity of human patients with HLH, we cannot claim that our model addresses all etiologic aspects of this disorder. However, this model is a powerful one because virtually every aspect of this diverse disorder is recreated in these mice. Furthermore, this model has already revealed 2 intriguing targets for clinical intervention in patients with HLH. While excellent progress has been made in the treatment of this disorder during the last decade, future progress will probably depend on further understanding of this still-fatal disorder.

## Acknowledgments

The authors would like to acknowledge Dr Peter Henson for helpful discussions and Azzedine Dakhama for assistance with microscopy.

## References

- Henter JI, Arico M, Elinder G, Imashuku S, Janka G. Familial hemophagocytic lymphohistiocytosis: primary hemophagocytic lymphohistiocytosis. *Hematol Oncol Clin North Am*. 1998;12:417-433.
- Janka G, Imashuku S, Elinder G, Schneider M, Henter JI. Infection- and malignancy-associated hemophagocytic syndromes: secondary hemophagocytic lymphohistiocytosis. *Hematol Oncol Clin North Am*. 1998;12:435-444.
- Favara BE, Feller AC, Pauli M, et al. Contemporary classification of histiocytic disorders. The WHO Committee On Histiocytic/Reticulum Cell Proliferations. Reclassification Working Group of the Histiocyte Society. *Med Pediatr Oncol*. 1997;29:157-166.
- Henter JI, Elinder G, Ost A. Diagnostic guidelines for hemophagocytic lymphohistiocytosis. The FHL Study Group of the Histiocyte Society. *Semin Oncol*. 1991;18:29-33.
- Ohga S, Matsuzaki A, Nishizaki M, et al. Inflammatory cytokines in virus-associated hemophagocytic syndrome: interferon-gamma as a sensitive indicator of disease activity. *Am J Pediatr Hematol Oncol*. 1993;15:291-298.
- Henter JI, Elinder G, Soder O, Hansson M, Andersson B, Andersson U. Hypercytokinemia in familial hemophagocytic lymphohistiocytosis. *Blood*. 1991;78:2918-2922.
- Akashi K, Hayashi S, Gondo H, et al. Involvement of interferon-gamma and macrophage colony-stimulating factor in pathogenesis of haemophagocytic lymphohistiocytosis in adults. *Br J Haematol*. 1994;87:243-250.
- Fujiwara F, Hibi S, Imashuku S. Hypercytokinemia in hemophagocytic syndrome. *Am J Pediatr Hematol Oncol*. 1993;15:92-98.
- Takada H, Ohga S, Mizuno Y, et al. Oversecretion of IL-18 in haemophagocytic lymphohistiocytosis: a novel marker of disease activity. *Br J Haematol*. 1999;106:182-189.
- Egeler RM, Shapiro R, Loechelt B, Filipovich A. Characteristic immune abnormalities in hemophagocytic lymphohistiocytosis. *J Pediatr Hematol Oncol*. 1996;18:340-345.
- Schneider EM, Lorenz I, Muller-Rosenberger M, Steinbach G, Kron M, Janka-Schaub GE. Hemophagocytic lymphohistiocytosis is associated with deficiencies of cellular cytolysis but normal expression of transcripts relevant to killer-cell-induced apoptosis. *Blood*. 2002;100:2891-2898.
- de Saint Basile G, Fischer A. The role of cytotoxicity in lymphocyte homeostasis. *Curr Opin Immunol*. 2001;13:549-554.
- Stapp SE, Dufourcq-Lagelouse R, Le Deist F, et al. Perforin gene defects in familial hemophagocytic lymphohistiocytosis. *Science*. 1999;286:1957-1959.
- Goransdotter Ericson K, Fadeel B, Nilsson-Ardnor S, et al. Spectrum of perforin gene mutations in familial hemophagocytic lymphohistiocytosis. *Am J Hum Genet*. 2001;68:590-597.
- Russell JH, Ley TJ. Lymphocyte-mediated cytotoxicity. *Annu Rev Immunol*. 2002;20:323-370.
- Shresta S, Pham CT, Thomas DA, Graubert TA, Ley TJ. How do cytotoxic lymphocytes kill their targets? *Curr Opin Immunol*. 1998;10:581-587.
- Binder D, van den Broek MF, Kagi D, et al. Aplastic anemia rescued by exhaustion of cytokine-secreting CD8<sup>+</sup> T cells in persistent infection with lymphocytic choriomeningitis virus. *J Exp Med*. 1998;187:1903-1920.
- Matloubian M, Suresh M, Glass A, et al. A role for perforin in downregulating T-cell responses during chronic viral infection. *J Virol*. 1999;73:2527-2536.
- Buchmeier MJ, Welsh RM, Dutko FJ, Oldstone MB. The virology and immunobiology of lymphocytic choriomeningitis virus infection. *Adv Immunol*. 1980;30:275-331.
- Ahmed R, Salmi A, Butler LD, Chiller JM, Oldstone MB. Selection of genetic variants of lymphocytic choriomeningitis virus in spleens of persistently infected mice: role in suppression of cytotoxic T lymphocyte response and viral persistence. *J Exp Med*. 1984;160:521-540.
- Wysocka M, Kubin M, Vieira LQ, et al. Interleukin-12 is required for interferon-gamma production and lethality in lipopolysaccharide-induced shock in mice. *Eur J Immunol*. 1995;25:672-676.
- Lochner M, Wagner H, Classen M, Forster I. Generation of neutralizing mouse anti-mouse IL-18 antibodies for inhibition of inflammatory responses in vivo. *J Immunol Methods*. 2002;259:149-157.
- Lochner M, Forster I. Anti-interleukin-18 therapy in murine models of inflammatory bowel disease. *Pathobiology*. 2002;70:164-169.
- Murayama T, Yokode M, Kataoka H, et al. Intra-peritoneal administration of anti-c-fms monoclonal antibody prevents initial events of atherogenesis but does not reduce the size of advanced lesions in apolipoprotein E-deficient mice. *Circulation*. 1999;99:1740-1746.
- Cook AD, Braine EL, Campbell IK, Rich MJ, Hamilton JA. Blockade of collagen-induced arthritis post-onset by antibody to granulocyte-macrophage colony-stimulating factor (GM-CSF): requirement for GM-CSF in the effector phase of disease. *Arthritis Res*. 2001;3:293-298.
- Parekh BS, Buchmeier MJ. Proteins of lymphocytic choriomeningitis virus: antigenic topography of the viral glycoproteins. *Virology*. 1986;153:168-178.
- Crowley M, Inaba K, Witmer-Pack M, Steinman RM. The cell surface of mouse dendritic cells: FACS analyses of dendritic cells from different tissues including thymus. *Cell Immunol*. 1989;118:108-125.
- Crawford F, Kozono H, White J, Marrack P, Kappler J. Detection of antigen-specific T cells with multivalent soluble class II MHC covalent peptide complexes. *Immunity*. 1998;8:675-682.
- Henter JI, Elinder G, Soder O, Ost A. Incidence in Sweden and clinical features of familial hemophagocytic lymphohistiocytosis. *Acta Paediatr Scand*. 1991;80:428-435.
- Orange JS, Biron CA. An absolute and restricted requirement for IL-12 in natural killer cell IFN-gamma production and antiviral defense: studies of natural killer and T cell responses in contrasting viral infections. *J Immunol*. 1996;156:1138-1142.
- Pien GC, Nguyen KB, Malmgaard L, Satooskar AR, Biron CA. A unique mechanism for innate cytokine promotion of T cell responses to viral infections. *J Immunol*. 2002;169:5827-5837.
- Zajac AJ, Blattman JN, Murali-Krishna K, et al. Viral immune evasion due to persistence of activated T cells without effector function. *J Exp Med*. 1998;188:2205-2213.
- Ou R, Zhou S, Huang L, Moskophidis D. Critical role for alpha/beta and gamma interferons in persistence of lymphocytic choriomeningitis virus by clonal exhaustion of cytotoxic T cells. *J Virol*. 2001;75:8407-8423.
- Baldrige JR, Buchmeier MJ. Mechanisms of antibody-mediated protection against lymphocytic choriomeningitis virus infection: mother-to-baby transfer of humoral protection. *J Virol*. 1992;66:4252-4257.
- Baldrige JR, McGraw TS, Paoletti A, Buchmeier MJ. Antibody prevents the establishment of persistent arenavirus infection in synergy with endogenous T cells. *J Virol*. 1997;71:755-758.
- Zinkernagel RM, Planz O, Ehl S, et al. General and specific immunosuppression caused by anti-viral T-cell responses. *Immunol Rev*. 1999;168:305-315.



37. Hermans IF, Ritchie DS, Yang J, Roberts JM, Ronchese F. CD8<sup>+</sup> T cell-dependent elimination of dendritic cells in vivo limits the induction of anti-tumor immunity. *J Immunol.* 2000;164:3095-3101.
38. Sambhara S, Switzer I, Kurichh A, et al. Enhanced antibody and cytokine responses to influenza viral antigens in perforin-deficient mice. *Cell Immunol.* 1998;187:13-18.
39. Kagi D, Odermatt B, Mak TW. Homeostatic regulation of CD8<sup>+</sup> T cells by perforin. *Eur J Immunol.* 1999;29:3262-3272.
40. Badovinac VP, Hamilton SE, Harty JT. Viral infection results in massive CD8<sup>+</sup> T cell expansion and mortality in vaccinated perforin-deficient mice. *Immunity.* 2003;18:463-474.
41. Tay CH, Welsh RM. Distinct organ-dependent mechanisms for the control of murine cytomegalovirus infection by natural killer cells. *J Virol.* 1997;71:267-275.
42. Topham DJ, Cardin RC, Christensen JP, Brooks JW, Belz GT, Doherty PC. Perforin and Fas in murine gammaherpesvirus-specific CD8(+) T cell control and morbidity. *J Gen Virol.* 2001;82:1971-1981.
43. Kagi D, Hengartner H. Different roles for cytotoxic T cells in the control of infections with cytopathic versus noncytopathic viruses. *Curr Opin Immunol.* 1996;8:472-477.
44. Topham DJ, Tripp RA, Doherty PC. CD8<sup>+</sup> T cells clear influenza virus by perforin or Fas-dependent processes. *J Immunol.* 1997;159:5197-5200.
45. Liu B, Mori I, Hossain MJ, Dong L, Chen Z, Kimura Y. Local immune responses to influenza virus infection in mice with a targeted disruption of perforin gene. *Microb Pathog.* 2003;34:161-167.
46. Heise MT, Connick M, Virgin HW 4th. Murine cytomegalovirus inhibits interferon gamma-induced antigen presentation to CD4 T cells by macrophages via regulation of expression of major histocompatibility complex class II-associated genes. *J Exp Med.* 1998;187:1037-1046.
47. LoPiccolo DM, Gold MC, Kavanagh DG, Wagner M, Koszinowski UH, Hill AB. Effective inhibition of K(b)- and D(b)-restricted antigen presentation in primary macrophages by murine cytomegalovirus. *J Virol.* 2003;77:301-308.
48. Snoeck HW, Van Bockstaele DR, Nys G, et al. Interferon gamma selectively inhibits very primitive CD34<sup>+</sup>CD38<sup>-</sup> and not more mature CD34<sup>+</sup>CD38<sup>+</sup> human hematopoietic progenitor cells. *J Exp Med.* 1994;180:1177-1182.
49. Mosser DM. The many faces of macrophage activation. *J Leukoc Biol.* 2003;73:209-212.